The active site of yeast phosphatidylinositol synthase Pis1 is facing the cytosol

Arlette Bochud, Andreas Conzelmann *

Department of Biology, University of Fribourg, Switzerland

Five yeast enzymes synthesizing various glycerophospholipids belong to the CDP-alcohol phosphatidyltransferase (CAPT) superfamily. They only share the so-called CAPT motif, which forms the active site of all these enzymes. Bioinformatic tools predict the CAPT motif of phosphatidylinositol synthase Pis1 as either ER luminal or cytosolic. To investigate the membrane topology of Pis1, unique cysteine residues were introduced into either native or a Cys-free form of Pis1 and their accessibility to the small, membrane permeating alkylating reagent N-ethylmaleimide (NEM) and mass tagged, non-permeating maleimides, in the presence and absence of non-denaturing detergents, was monitored. The results clearly point to a cytosolic location of the CAPT motif. Pis1 is highly sensitive to non-denaturing detergent, and low concentrations (0.05%) of dodecylmaltoside change the accessibility of single substituted Cys in the active site of an otherwise cysteine free version of Pis1. Slightly higher detergent concentrations inactivate the enzyme. Removal of the ER retrieval sequence from (wt) Pis1 enhances its activity, again suggesting an influence of the lipid environment. The central 84% of the Pis1 sequence can be aligned and fitted onto the 6 transmembrane helices of two recently crystallized archaeal members of the CAPT family. Results delineate the accessibility of different parts of Pis1 in their natural context and allow to critically evaluate the performance of different cysteine accessibility methods. Overall the results show that cytosolically made inositol and CDP-diacylglycerol can access the active site of the yeast PI synthase Pis1 from the cytosolic side and that Pis1 structure is strongly affected by mild detergents.
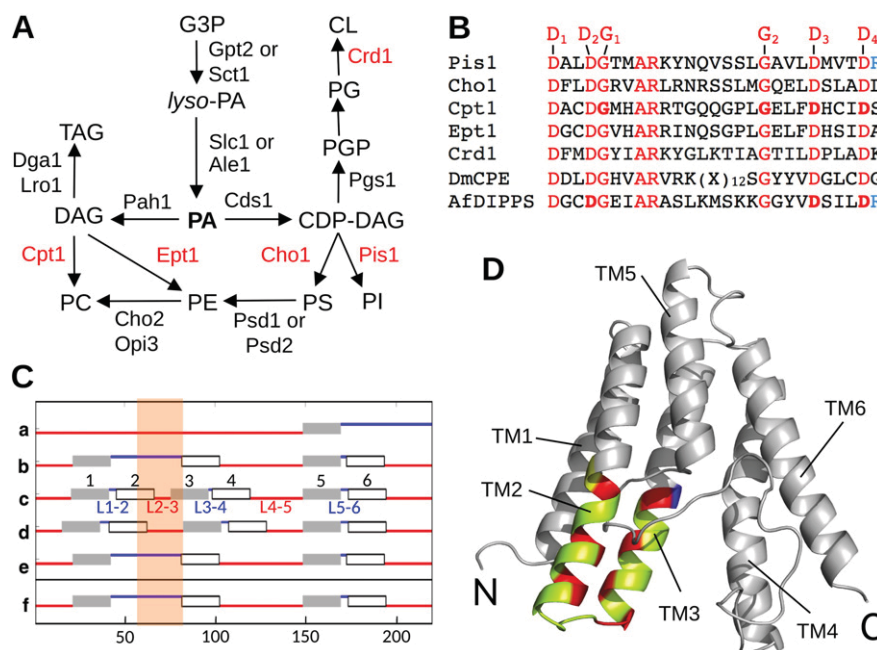
1. Introduction

Many eukaryotic lipids are made from phosphatidic acid (PA), which is transformed into CDP-diacylglycerol (CDP-DAG) to be used for synthesis of phosphatidylinositol (PI), phosphatidylserine (PS), phosphatidylglycerolphosphate (PGP), and cardiolipin (CL) by the respective enzymes Pis1, Cho1, Pgs1, and Crd1 (Fig. 1A) [1]. Pah1 can dephosphorylate PA to diacylglycerol (DAG), which can be utilized by the so-called Kennedy pathway enzymes Cpt1 or Ept1 to form phosphatidylcholine (PC) and phosphatidylethanolamine (PE), respectively (Fig. 1A). *PIS1*, *CHO1*, *CPT1*, *EPT1* and *CRD1* all belong to the CDP-alcohol phosphatidyltransferase (CAPT) cl00453 superfamily and pfam01066 family, the members of which have the ability to catalyze the displacement of CMP from a CDP-alcohol by a second alcohol, thus creating a phosphodiester bridge between two alcohols. A wide range of substrates is used by different CAPT proteins and their sequences can be very different, but they all share the 25–30 amino acid long conserved CAPT motif $D(X_2)DG(X_2)AR(X_{7-12})G(X_3)D(X_3)D$ [2] (Fig. 1B).

High resolution crystal structures have recently been reported for two CAPTs of the hyperthermophilic Archaeon *Archaeoglobus fulgidus*, one of unknown specificity, the other being a di-*myo*-inositol-1,3-phosphate-1′-phosphate synthase (AfDIPPS) catalyzing the condensation of two hydrophilic alcohols, CDP-inositol and inositol-1-phosphate [3,4]. Crystals show a novel fold formed by 6 transmembrane helices (TMs) forming a polar cavity extending from the cytosol to a depth of 8 Å into the membrane [4]. As shown in Fig. 1D, when Pis1 is modeled on the AfDIPPS protein, the CAPT motif occupies the C-terminal end of TM2, the connecting loop L2–3 and the N-terminus of TM3, as it does in the AfDIPPS itself [4]. The whole CAPT motif is lining one side of the polar cavity. The co-crystallization of one CAPT with CDP and CMP allowed to show that D_1, D_2 and D_3 of the CAPT motif coordinate the pyro-phosphate of CDP via a divalent cation and that the planar cytidine ring is inserted between G_1 and the conserved A 3 positions further down on the one hand, G_2 on the other hand (Fig. 1B) [3]. Thus, it is beyond doubt that the CAPT motif is part of the active site. D_4 of the CAPT motif is proposed to act as a catalytic base, deprotonating the second substrates' alcohol to allow its attack on the β-phosphate of CDP [3].

We became interested in the topology of glycerophospholipid biosynthesis in the ER because there is evidence that in yeast, PA can be generated at the luminal side of the ER membrane although the substrates for this biosynthesis are made in the cytosol [5,6]. While Pah1 is a

* Corresponding author at: University of Fribourg, Department of Biology, Chemin du Musée 10, CH-1700 Fribourg, Switzerland. Tel.: +41 26 300 8630; fax: +41 26 300 9735.
E-mail address: Andreas.Conzelmann@unifr.ch (A. Conzelmann).

Fig. 1. CAPT enzymes involved in glycerophospholipid biosynthesis. A, the yeast enzymes belonging to the CAPT family (pfam01066) are marked in red. Pgs1 also uses CDP-DAG but belongs to another, distantly related CAPT family. B, the conserved CAPT motif of the 5 CAPT family members of yeast, *D. melanogaster* ceramide phosphoethanolamine synthase (DmCPE) and AfDIPPS. Substitution by Ala of residues in bold leads to complete loss of activity (Willams and McMaster, 1998). Absolutely conserved D and G residues of the CAPT motif are numbered as in [4]. CAPTs using Ino-containing substrates conserve an R (blue) after D_4. C, TOPCONS prediction for Pis1 (October 2014). Color code: red are cytosolic, blue are luminal loops; grey and white boxes delimitate TMs. Lines a–e represent topology predicted by SCAMPI-seq, SCAMPI-msa, PRODIV, PRO and OCTOPUS algorithms. Line f represents the final TOPCONS prediction taking into account a–e plus two further algorithms. The orange rectangle delineates the position of the CAPT motif. D, The peptide backbone of yeast Pis1 was modeled based on the crystal structure of AfDIPPS as described in Materials and methods [4]. Unaligned amino acids 1–15 and 201–220 are not shown. The CAPT motif is in light green; its conserved residues are in red and blue as in panel B.

cytosolic enzyme, all other enzymes shown in Fig. 1A are integral membrane proteins. So far no crystal structures are reported for any of them, nor for homologs in other species, except for the two archeal structures mentioned above, but recent biochemical studies in yeast have provided some information on the probable active site orientation for Gpt2, Slc1, Ale1, Lro1, Dga1 and the mitochondrial Psd1 [5–9], the first 5 proposing ER luminal orientation of the most conserved polar residues. As for CAPTs, a novel CDP-ethanolamine-dependent ethanolamine-phosphoceramide synthase of *Drosophila melanogaster* belonging to the pfam01066 family has its catalytic site and its CAPT motif in the lumen of the Golgi (Fig. 1B) [10].

TOPCONS and Phobius are amongst the most popular bioinformatic topology predictors; TOPCONS uses 7 independent algorithms and integrates them into a final topology prediction, which in 75–80% of cases is correct [11] (http://topcons.net/). For Pis1, TOPCONS algorithms are unanimous only with regard to one single TM, TM5 and the loops preceding and following it (L4–5 and L5–6). The integrated final prediction places the CAPT motif of Pis1 into the ER lumen (Fig. 1C, line f). Phobius predicts 3 TMs and all connecting loops have about equal probability to be luminal or cytosolic (Fig. S1). As for AfDIPPS, its active site is cytosolic. This was not deduced from the crystal structure but comes from independent biochemical evidence [12]. Inositol (Ino), serine, CDP-choline and CDP-ethanolamine all are synthesized in the cytosol. However, a wealth of literature demonstrates that glycerophospholipids in rat liver microsomes flip flop very rapidly, with half-times of tens of seconds, that their flip flop is bidirectional, ATP-independent but protein dependent, since it can be blocked by protein modifying reagents or protease treatment, and can be reconstituted into proteoliposomes [13]. The same has also been found for yeast microsomes [14]. Inositol and, according to unanimous TOPCON predictions, probably also CDP-DAG (Fig. S2F) are made in the cytosol or on the cytosolic side of the ER membrane, but this does not in itself allow the conclusion that PI synthesis has to occur on the cytosolic side of the ER membrane.

The uncertainty about the orientation of Pis1 motivated us to investigate its topology biochemically.

2. Results

2.1. Two types of substituted cysteine accessibility methods (SCAM) were used

SCAM has widely been used to determine the topology of membrane proteins. Classically it uses NEM or derivatives of it as the alkylating group. In order to react with NEM, a Cys has to be deprotonated to the thiolate and the reaction therefore occurs rapidly only with Cys that are in contact with water (Fig. S3A). Thus, SCAM distinguishes 3 categories of Cys in membrane proteins: those at the water-accessible surfaces, either cytosolic or luminal, and those "buried" in the water-free zones inside the protein or the lipid bilayer. In all SCAM experiments we used bulky non-permeating NEM derivatives, either methoxypolyethylene glycol$_{5000}$-maleimide (PEG-mal) [15] or ubiquitin-maleimide (Ub-mal) [5] (Fig. S3B, D). Both reagents, when reacting with a free Cys on a target protein, cause a molecular weight increase that can be seen in Western blots. We used Ub-mal because PEG-mal was shown to penetrate yeast microsomal membranes and derivatize the soluble, ER luminal Kar2 protein, albeit only at room temperature (RT), not at 4 °C [6]. Also, PEG-mal partitions well into organic solvents of intermediate dielectric constants ($4.5 < \varepsilon < 10$), which are routinely used to extract membrane lipids (Fig. S4). As for Ub-mal, we estimated that only the spacer between ubiquitin and the maleimide could potentially reach into the membrane (Fig. S3B). In order to see if Cys residues are situated at the surface of Pis1 or rather in water-filled pockets, we coupled maleimide to ubiquitin using spacers of different length (Fig. S3B, C).

Two different SCAM methods were utilized [16]. One approach compares Cys derivatization by membrane non-permeating bulky alkylating reagents added to either intact or detergent-permeabilized microsomes

[5,15]. For this we used Ub-mals and n-dodecyl-β-D-maltoside (DDM) and therefore refer to this approach as Ub-mal/DDM method. The examples shown in Fig. 2A demonstrate that the Ub-mal/DDM method allows to distinguish cytosolic, luminal and non-accessible Cys residues. All experiments used cells also expressing FLAG-Gpi8, a single span luminal ER protein containing four Cys, at least two of which are accessible in microsomes in the presence of 0.05% DDM, but not in the absence of detergent (Fig. 2A). This control attested that microsomes were intact.

Examples of the 3 types of results obtained with the other approach are shown in Fig. 2B. In this approach one considers as cytosolic those Cys that in native microsomes are modified by PEG-mal, as luminal those Cys that in native microsomes are modified by the membrane permeating NEM but not by PEG-mal, and as buried those Cys that in native microsomes are modified by neither, but can be accessed by PEG-mal in the presence of SDS (Fig. 2B). Residues are classified as "partially buried" when, as in Fig. 2B, bottom panel, derivatization of a residue in the presence of SDS is not completely inhibited by preincubation with NEM at 0.3 or 5 mM. We refer to this approach as PEG-mal/NEM method [8,17]. Therein one also can assess microsome integrity using Gpi8 (Fig. 2B).

2.2. Preparation of cysteine free forms of Pis1 for SCAM

Pis1 contains 5 native Cys at positions 53, 90, 93, 100 and 154. The substitution of residues by Cys for SCAM can potentially change the conformation of a protein and increase or decrease the accessibility of its native Cys. To be on the safe side we decided to place a Cys-free version of Pis1 (Pis1ΦC) behind the galactose inducible GAL1 promoter and to introduce single Cys at various sites into it, thereby eliminating any doubts about the identity of a derivatized residue. Thus, the five native Cys of Pis1, all being part of rather hydrophobic sequences, were mutated to alanine by site-directed mutagenesis. Pis1ΦC could not be derivatized with any mass tagged maleimide, even in the presence of SDS as expected (see below, Fig. 5D). Thereafter, single non-conserved residues located in hydrophilic loops predicted by TOPCONS (Fig. 1C) were mutated to Cys to generate new Pis1 alleles having one single Cys.
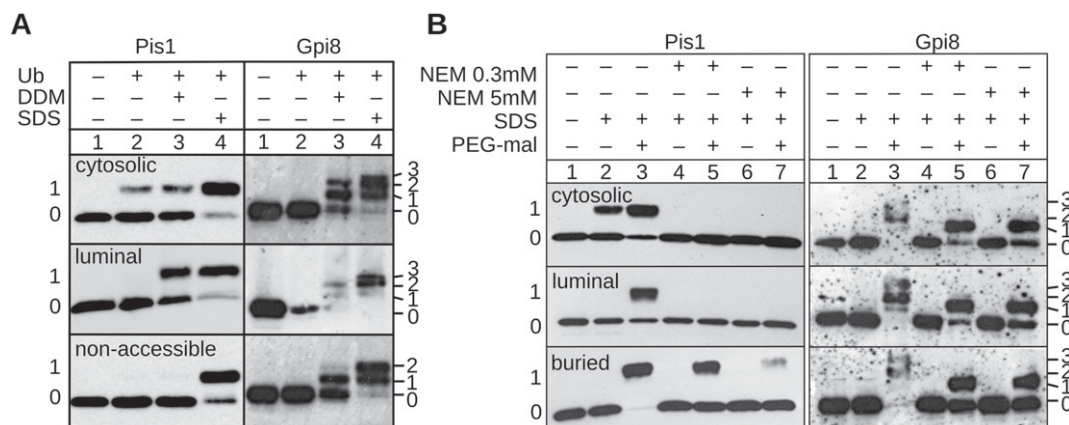
Topologies established for enzymes are considered relevant if obtained from enzymatically active alleles. Functionality of the plasmid-borne constructs was verified by transfection of the plasmids into pis1Δ/PIS1 heterozygous diploids and tetrad dissection. All constructs tested yielded four viable spores on galactose, indicating the constructs' ability to rescue the lethal pis1Δ::kanMX4 deletion in the haploid offspring. We further monitored the ability of the various complemented pis1Δ strains to grow on glucose, raffinose, or galactose (Fig. 3A).

Expression of PIS1ΦC allowed some growth on glucose (Fig. 3A, dotted red line) albeit less than expression of wild type (wt) PIS1 (red line). Some Xxx ⇒ Cys mutations in PIS1ΦC resulted in worse (blue lines), others in normal or even improved growth on glucose (grey lines). On raffinose or galactose, most mutant alleles restored normal growth (Fig. 3A). Pis1Δ cells harboring wt PIS1 (Fig. 3A, red line) grew slightly less rapidly than wt cells harboring empty vector (green line) on both galactose, and glucose, suggesting that even slight overexpression of Pis1 may be suboptimal, possibly because Pis1 and Cho1 are in competition with each other for CDP-DAG when cells, as here, are cultured in complete synthetic medium containing 400 μM Ino [18].
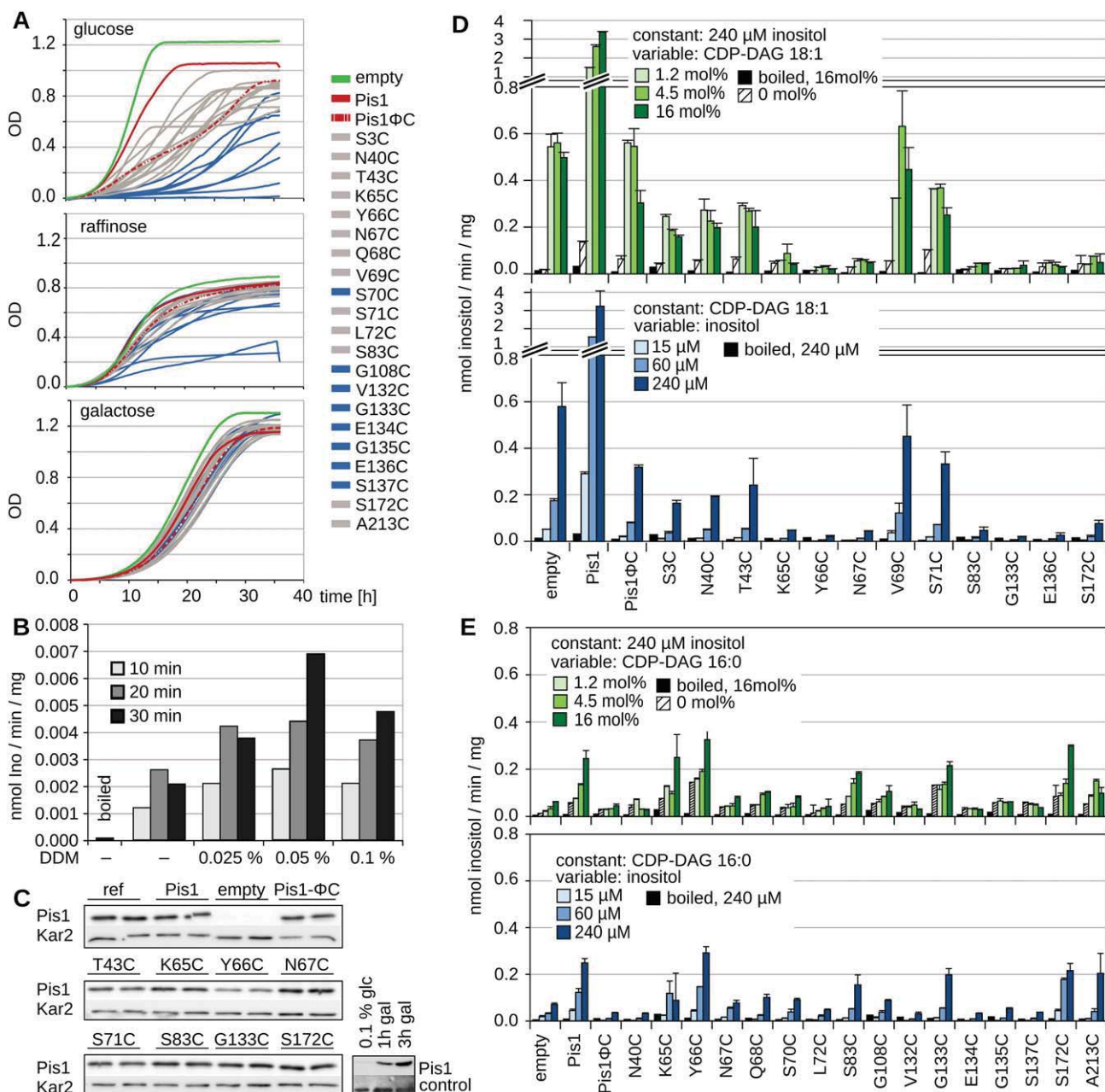
2.3. In vitro activity of Pis1ΦC constructs

To better quantify Pis1 activity we used an in vitro assay modified from [19], wherein cell extracts were incubated with cold CDP-DAG plus [^{3}H]Ino. Here we however used microsomes, prepared exactly as for SCAM, and assayed Pis1 activity at pH 7.2, the pH used for SCAM, rather than pH 8.0. Preliminary assays showed that microsomes prepared from spheroplasts were superior to microsomes obtained by glass bead fragmentation of cells (Fig. S5A). Other preliminary data indicated that several non-ionic, i.e. "mild" detergents strongly reduced Pis1 activity at concentrations > 0.1% (Fig. S5B). Further experiments also showed that lower concentrations of detergent could stimulate microsomal activity as observed before [20], the optimal concentration for DDM being 0.05% (w/v). This corresponds to an estimated molar DDM:lipid ratio of about 1.5 (Fig. 3B) (see supplemental materials and methods for calculation of detergent:lipid ratios and mol.% of lipids). The reactions were usually linear with time up to 20–30 min (Figs. 3B; S5C) and with increasing Ino concentrations up to 240 μM Ino (Fig. 3D, lower panel), which roughly corresponds to the K_M of the purified enzyme for Ino [21]. Reactions with wt microsomes (empty plasmid) seemed to be close to saturation with 24 μM (1.2 mol.%) CDP-DAG (Fig. 3D, upper panel). Based on these preliminary assays we established two standard protocols, in which one of the substrates was kept constant and the other one was varied. Thus, all PIS1 alleles used for SCAM were assayed as shown in Fig. 3D or E. In all enzyme assays, activities were normalized with regard to Pis1 protein detectable in Western blots (Fig. 3C) as detailed in supplemental materials and methods. Indeed, as shown in Fig. 3C, apart from a few exceptions, most mutant Pis1 proteins were stable.

Fig. 2. Typical results obtained using different SCAM methodologies. Panel A and B, microsomes from cells expressing FLAG-Gpi8 and Pis1-V5-His6 alleles having one single Cys residue were subjected to SCAM using either the Ub-mal/DDM method (A) or the PEG-mal/NEM method (B). Pis1 and Gpi8 were detected on western blots with anti-V5 and anti-FLAG antibodies, respectively. In each case a typical example of a cytosolic (top), a luminal (middle) and a non-accessible (A) or a buried (B) Cys (bottom) was chosen. Numbers 0, 1, 2, and 3 on the right side indicate the number of PEG-mals attached to Gpi8. Absence of derivatization in lanes 2 of FLAG-Gpi8 blots shows that the microsomes were intact. A, Ub = Ub-mal. Lane 3 shows that two Cys of Gpi8 are easily accessible for Ub-mals in the presence of 0.05% DDM (top and bottom) or 1% DDM (middle). However, one of the 4 Cys of Gpi8 remains inaccessible even in SDS. B, the panel at the bottom actually shows a Cys that is only partially buried.
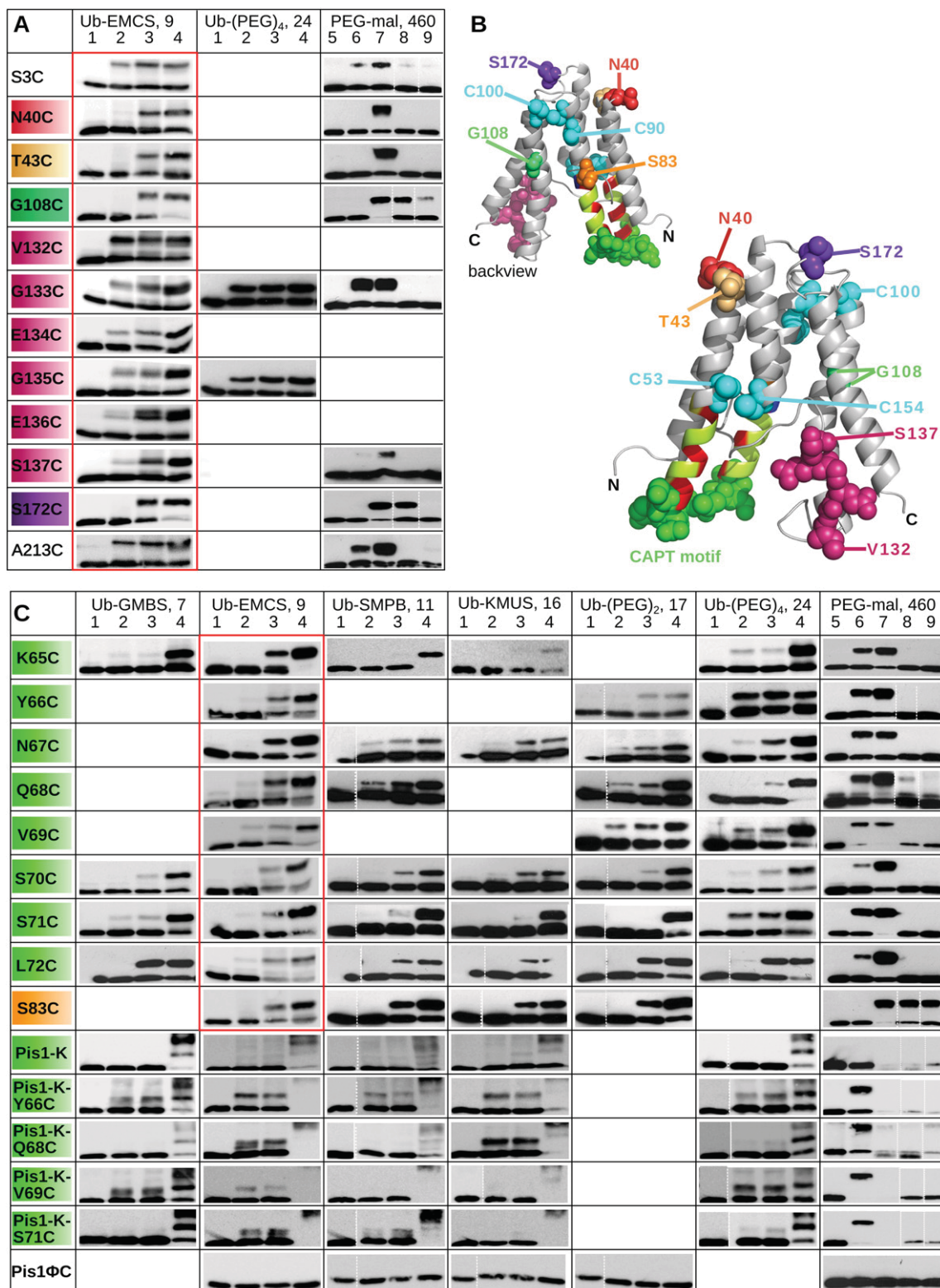
Fig. 3. Cysteine substitutions in Pis1ΦC. A, growth curves of *pis1Δ* strains carrying plasmids with the indicated Pis1ΦC alleles in galactose, raffinose and glucose at 30 °C. Green: WT cells + empty vector (empty), red: *pis1Δ* + Pis1-V5-His6, dashed red: *pis1Δ* + Pis1ΦC-V5-His6, blue: strains growing slow on glucose. Curves represent average of 6 cultures, two independent meiotic segregants, each assayed in triplicate. B, 100 μg of microsomes from *pis1Δ* + Pis1-V5-His6 cells induced for 30 min was incubated with 1 μCi of [³H]Ino for 10–30 min, in the presence of 0–0.1% DDM, 10 μM (0.6 mol.%) CDP-DAG 18:1 and 0.25 μM Ino. C, typical Western blots for relative quantification of Pis1ΦC-V5-His6 variants in the microsomes used for the activity assays; 5 μg/lane, probed by anti-V5-HRP and anti-Kar2. Inset: 1 h and 3 h induction of Pis1-V5-His6 after adding 2% galactose to an overnight culture in 0.1% glucose. D and E, enzymatic activity of *pis1Δ* + Pis1ΦC-derived variants in the presence of CDP-DAG 18:1 (D) and CDP-DAG 16:0 (E), with a constant concentration of Ino (240 μM; green) or of CDP-DAG (307 μM, *i.e.* 16 mol.%; blue). Incorporation of Ino into lipids was normalized with regard to amounts of Pis1 protein (panel C) present in the microsomes (see supplemental materials and methods). The mean and deviations from the mean of duplicate assays of microsomal preparations are reported.

During this study we used two different commercially available CDP-DAG versions, CDP-DAG having C18:1 fatty acids and CDP-DAG having C16:0. Neither of them corresponds to the natural substrate, which probably has C16:0 in sn1 and C18:1 in sn2. We found that: 1) Wt Pis1 at its physiological expression level (empty vector) as well as overexpressed Pis1ΦC had comparatively good activity with CDP-DAG C18:1 but much less with CDP-DAG C16:0 (Fig. 3D vs. E, green panels). 2) The K_M for CDP-DAG C16:0 of wt Pis1 at its physiological expression level (empty vector) seemed to be higher than the one for CDP-DAG C18:1 (Fig. 3D vs. E, green panels, "empty" (vector)).

3) Pis1ΦC had about 3–9 fold lower activity than wt Pis1 (Fig. 3D, E). 4) Most of the Cys substitutions in the Pis1ΦC molecule that were tested with CDP-DAG C18:1 showed similar or lower activity than the parental Pis1ΦC protein, whereas amongst those tested with CDP-DAG C16:0, Cys substituted version tended to have the same or higher activity than the parental Pis1ΦC (Fig. 3D vs. E). This could also be seen for those Cys-substituted Pis1ΦC versions that were tested with both substrates, CDP-DAG C16:0 and CDP-DAG C18:1 (Fig. S6). Thus, data suggest that replacement of a polar residue by Cys at several places in the protein caused a preference for CDP-DAGs with shorter and more

4

saturated fatty acids. 5) After 30 min of induction with galactose, the microsomes of *pis1Δ* harboring wt Pis1 had 5 fold higher than the physiological Pis1 activity present in wt cells having empty vector (Figs. 3D, E, S6). 6) Quite comparable results were also obtained when [CDP-DAG] rather than [Ino] was kept constant (Fig. 3D, E, lower, blue panels).

Fig. 4. Western blots of SCAMs for Pis1ΦC and Pis1-K variants. A, Cys substitutions outside the CAPT motif made in Pis1ΦC-V5-His6. Experiments using Ub-mal/DDM (lanes 1–4) and PEG-mal/NEM method (lanes 5–9) are shown. Lanes 1: control, lanes 2: Ub-mal, lanes 3: Ub-mal/DDM, lanes 4: Ub-mal/SDS as in Fig. 2A. DDM was added to 0.05% except for experiments encircled by a red line, for which 1% was used. Lanes 5: control, lanes 6: PEG-mal, lanes 7: PEG-mal/SDS, lanes 8: 0.3 mM NEM, then PEG-mal/SDS, lanes 9: 5 mM NEM, then PEG-mal/SDS. B, model of Pis1 aligned to AfDIPPS as in Fig. 1D, small back and large front views. The positions of the substitutions and of the five native Cys are highlighted by colored spheres. Light green: the CAPT motif, with strictly conserved residues in red and blue, and the substituted residues K65 to L72 as bright green spheres. C, Cys substitutions inside the CAPT motif made in Pis1ΦC (upper part) and Pis1-K (lower part), starting from the smallest linker (GMBS, 7 Å) on the left to the longest (PEG-mal, 460 Å) on the right, with the length of linker given in Å on top. Lanes 1–9 as in A.

5

Thus, all Cys-free and Cys-substituted Pis1 alleles described above could support growth of *pis1Δ* cells, at least when overexpressed, and also had some *in vitro* activity. We therefore decided to probe their topology using SCAM.

2.4. SCAM assays of single cysteines introduced into Pis1ΦC

The apparent molecular weight of Pis1-V5-His6 on SDS-PAGE is 30 kDa; after derivatization of a single Cys with Ub-mal or PEG-mal it is 35 and 40 kDa, respectively. Pis1ΦC-S3C could clearly be derivatized with Ub-EMCS and PEG-mal in the absence of detergent, indicating a cytosolic location of the N-terminus of Pis1ΦC (Fig. 4A). (All quantifications of derivatizations in Fig. 4 are shown in Fig. S7B, all control blots of Gpi8 assessing tightness of microsomes in Fig. S8). The cytosolic location of the N-terminus also is suggested by the fact that it is N-acetylated [22]. The position of the short loop L1–2 predicted by two algorithms of TOPCONS (lines c and d of Fig. 1C) was probed through the mutations N40C and T43C. In the absence of SDS, both were accessible to NEM but not to PEG-mal (Fig. 4A); they reacted with Ub-EMCS only in the presence of 1% DDM. (Only after having performed a first round of experiments with Ub-EMCS did we realize that DDM at 1% abolishes the Pis1 activity and therefore reduced DDM concentration to 0.05% for all subsequent experiments). Thus, data obtained by Ub-EMCS in the absence of detergent suggest that both residues are not cytosolic; the ones obtained with PEG-mal/NEM method clearly indicate a luminal position, a concept also supported by the model shown in Fig. 4B.

To probe the eight residues K65 to L72 residing in the poorly conserved region in the middle of the CAPT motif, many Cys substitutions were not only probed using the PEG-mal/NEM method but also Ub-mals of different spacer lengths (Fig. 4C). All data clearly point to the cytosolic location of the CAPT motif. The following tendencies could be observed: 1) In the absence of DDM, many Ub-mals with spacers shorter than 17 Å reacted poorly (see also Fig. S7B). 2) The Ub-SM(PEG)$_4$ (24 Å) allowed a more robust reaction in the absence of DDM in 3 out of 8, Ub-SM(PEG)$_2$ (17 Å) in 1 out of 7 substitutions. 3) Weak reactivity with Ub-SM(PEG)$_4$ in the absence of DDM correlated in two cases with relatively equally weak reactivity with PEG-mal (S70C and L72C), whereas weak reactivity of Q68C may be related to the fact that this residue is slightly buried. 4) Strikingly, in 25 out of 38 Ub-mal experiments in the CAPT region, addition of DDM strongly increased reactivity of substituted Cys. This phenomenon was not only observed in Ub-EMCS experiments, where we used 1% DDM, but also when only 0.05% DDM was added, including in experiments utilizing the longer SM(PEG) spacers (Figs. 4C or S7B). The findings suggest that detergent even at such low concentration has a major influence on the structure of the Pis1ΦC derivatives and in particular on the configuration of the CAPT domain. 5) Adjacent cytosolic residues can show very different accessibility, as may be expected in view of the various possible secondary structures (Fig. 4C, *e.g.* reactivities with Ub-SM(PEG)$_4$). 6) The luminal orientation of N40C/T43C and the cytosolic one of the CAPT motif suggest that TOPCONS algorithms PRODIV and PRO (lines c and d in Fig. 1C) are the only ones generating models compatible with our SCAM data and fitting the model of Figs. 1D and 4B.

S83C, next to R82 (blue in Fig. 1B for Pis1 and AfDIPPS), was not accessible to any Ub-mal nor PEG-mal in the absence of detergent (Fig. 4C, lanes 2) and NEM at 0.3 or 5 mM only accessed 22 and 34% of this site, respectively, because the bulk of Pis1ΦC-S83C could still be derivatized by PEG-mal after NEM treatment (Fig. 4C, lanes 8 and 9). This fits the model of Fig. 4B, which places S83 into the middle of TM3. Strikingly however, 0.05% DDM rendered this residue accessible to Ub-mals (Fig. 4C), arguing again that low amounts of detergent have major structural effects on Pis1ΦC. We speculate that 0.05% DDM may open up the access to S83C through the hydrophilic cytosolic cavity, implying that this access is partially blocked in its absence.

The G108C mutation was designed to probe the potential luminal loop L3–4 predicted by the TOPCONS PRO algorithm (line d in Fig. 1C).

In the absence of detergent it was inaccessible for Ub-EMCS and PEG-mal and was partially buried (Fig. 4A). Indeed, the model of Fig. 4B places it into the middle of TM4.

L4–5 is unanimously predicted as a cytosolic loop by TOPCONS (Fig. 1C) and as possibly having coil conformation by HHpred (http://toolkit.tuebingen.mpg.de/hhpred). Most positions, from V132 to S137 could be accessed by Ub-EMCS in the absence of detergent, the accessibility decreasing from V132C (43%) towards S137C (10%), a trend also visible when PEG-mal was utilized (64 vs. 3% of G133C and S137C, respectively) (Fig. S7B). This trend was abolished in the presence of DDM, whereby it has to be considered that 1% DDM (used in Ub-EMCS experiments) abolishes Pis1 activity and hence may partially denature the enzyme (see above). As neither G133C nor S137C is buried, the reduced reactivity of the C-terminal end of L4–5 may indicate some structural constraints and the model of Fig. 4B indeed suggests that S137 is already dipping below the membrane boundary.

The short loop L5–6 between TM5 and TM6 scores as luminal. A Cys placed at position 172 could be blocked partially and completely by 0.3 and 5 mM NEM, respectively, thereby indicating that it is partly accessible, but it was not accessible to PEG-mal and Ub-EMCS in the absence of detergent, consistent with a slightly buried luminal position.

The cytosolic location of the C terminus is indicated by the significant derivatization of A213C in the absence of detergent (48% by PEG-mal, 35% by Ub-EMCS (Figs. 4A, S7B)). A213C could be blocked by NEM to only about 90%, indicating that it might be slightly buried.
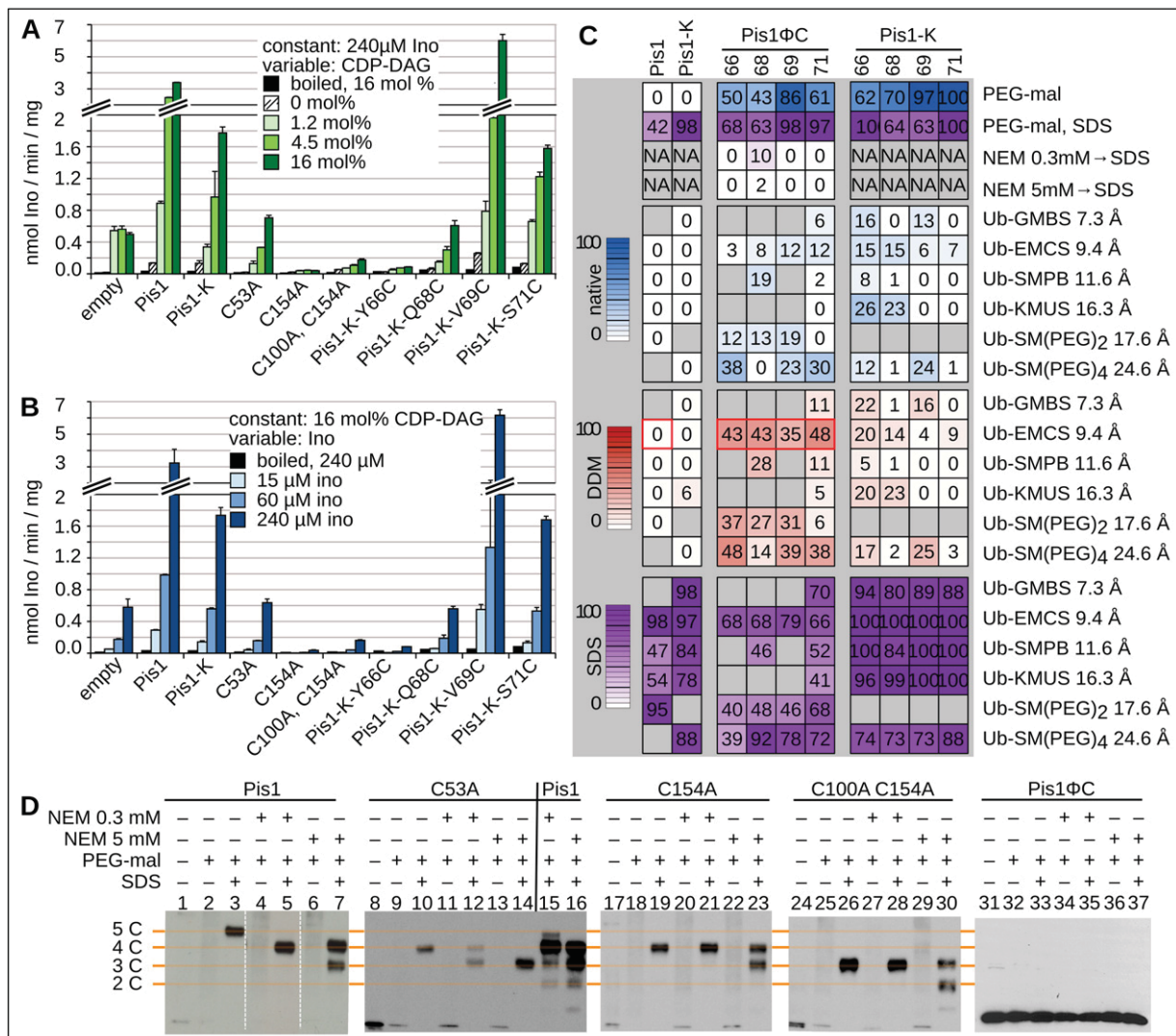
Thus, all SCAM data obtained from single Cys alleles support the model shown in Fig. 4B if we place its top part in the ER lumen, the bottom part in the cytosol.

2.5. SCAM assays of wild type Pis1

One way to explain the relatively low activity of Pis1ΦC and alleles derived thereof (Fig. 3D, E) is to presume that these alleles are partially folded into abnormal structures so that the enzymatic activity is carried by a minority of correctly folded proteins, whereas a majority of Pis1 proteins would be structurally abnormal. Under this assumption, SCAM studies using Pis1 alleles derived from Pis1-ΦC may mainly reveal the structure of abnormally structured proteins that are enzymatically dead. To avoid this potential error, we envisaged to transfer a few single substitutions made in the CAPT motif of Pis1ΦC to Pis1-V5-His6, still retaining the five native Cys. For this, we first wanted to understand if any of these native Cys would be derivatized during SCAM.

When Pis1-V5-His6 was subjected to SCAM analysis with PEG-mal, we found that 3 of its 5 native Cys were completely buried, one was accessible and another one was partially buried (Fig. 5D, lanes 1–7): 0.3 mM NEM blocked only one of the 5 Cys of Pis1, whereas 5 mM NEM partially blocked a second one (Fig. 5D, lanes 3, 5, 7). On the other hand, in the absence of SDS there were no discernible bands with one or two PEG substitutions in wt and Cys mutated Pis1 alleles tested, but a diffuse haze reaching even higher up than the species with all its Cys substituted was often visible (Fig. 5D, lanes 2, 4, 6, 9, 11, 13, 18, 20, 22 etc.). As samples were only heated but not boiled before SDS-PAGE, we presently presume that Pis1 was not completely soluble after heating in sample buffer unless SDS was already present during the assay. Similarly, no distinct bands corresponding to singly or doubly derivatized forms appeared after derivatization of microsomes containing wt Pis1 with Ub-mals (Fig. 4C, therein Pis1-K, see below). This argues that the small NEM can access certain Cys of wt Pis1, which are out of reach for mass tagged maleimides.

To identify these Cys residues, we examined different alleles, in which native Cys residues were deleted. In a C53A mutated Pis1, 0.3 mM NEM blocked one of the remaining 4 Cys, but 5 mM NEM could no more block a second Cys (Fig. 5D, lanes 10, 12, 14), suggesting that Cys53 was the partially accessible Cys residue requiring 5 mM NEM to be blocked. In a C154A mutated or a C154A_C100A doubly mutated version of Pis1, 0.3 mM NEM could not block any Cys, whereas 5 mM

Fig. 5. Analysis of variants derived from wild type Pis1 by removal or addition of single cysteines. A, B, microsomal Pis1 activity of *pis1*Δ cells harboring wt Pis1-V5-His6, or Pis1 with one or two native Cys changed to Ala (C53A, C154A, or both C100A and C154A), or Pis1-K variants having six Cys (Y66C, Q68C, V69C or S71C plus the five native Cys). Assays were done with constant concentrations of Ino (A) or CDP-DAG 18:1 (B) as in Fig. 3D. C, degree of derivatization of different alleles in different conditions in %. Top panel: PEG-mal/NEM method. Lower Panels, Ub-mal/DDM method. The squares color shaded in blue represent the derivatizations in the absence of detergent, squares shaded in red show derivatizations in the presence of DDM, and those shaded in purple derivatizations in the presence of SDS (1%). Grey cells: not tested or result discarded because microsomes were not tight. The experiments in which 1% DDM instead of 0.05% was used are framed in red. Percentages were calculated from data in Fig. 4C according to (Pis1$_{deriv.}$ / [Pis1$_{deriv.}$ + Pis1$_{non-deriv.}$]) × 100 (see Materials and methods), counting as "derivatized" only monosubstituted forms of Pis1, except for Pis1 alleles with 5 or 6 Cys derivatized in SDS: For those, all derivatized forms were counted. NA, not applicable. D, PEG-mal/NEM method was used to analyze Cys accessibility in wt Pis1 having 5 Cys and mutants with only 4, 3 or none of the native Cys. To increase resolution, the non-derivatized Pis1 was let run out of the gel.

still could partially block one of the remaining Cys (Fig. 5D, lanes 19, 21, 23 and 26, 28, 30). This strongly suggests that Cys154 is freely accessible to NEM and can easily be blocked by 0.3 mM NEM. The three buried Cys therefore are at positions 90, 93 and 100. None of the 5 Cys is disulfide bridged, since all 5 Cys of Pis1 were derivatized by PEG-mal in the presence of SDS (Fig. 5D, lane 3). (Note that zymolyase treatment of cells, preparation of microsomes, and derivatization assays were performed without reducing agents.)

Comparison of these results with the model created from the crystal structure of AfDIPPS (Fig. 4B), suggests that the proximity of Cys53 and Cys154 to the central cavity may explain why they can be derivatized by NEM. It should be noted that a major part of this cavity is occupied by side chains not visible on Fig. 4B. These side chains may hinder the access of mass tagged maleimides. Cys 90, 93 and 100 appear to be buried, although the model of Fig. 4B predicts them to be close to the luminal surface of Pis1. It is possible that their side chains point away from the water interface or that a peripheral membrane protein blocks access of NEM to these residues. When testing the enzymatic activity of

Pis1 alleles with one or two Cys ⇒ Ala mutations, we found that the C154A, or C154A/C100A double mutation alleles had less activity than Pis1ΦC lacking all 5 native Cys (Figs. 5A, B vs. 3D). Thus it appears that Cys to Ala substitutions, although relatively conservative, had major effects on enzyme activity, even though none of the 5 Cys of Pis1 seemed to be a critical active site residue, since Pis1ΦC was enzymatically active. However, Cys154 is conserved in Pis1 homologs of organisms as diverse as human, mouse, *Arabidopsis*, yeast and *Schizosaccharomyces pombe*, thus suggesting an important functional role for this residue.

2.6. SCAM assays of single cysteines introduced into the CAPT motif of wild type Pis1

The C-terminal V5-His6 tag added to Pis1 and Pis1ΦC inactivated the natural C-terminal KXKXX ER retrieval motif in the constructs used above. In the Cys substitutions in wt Pis1 alleles to be constructed, the KXKXX motif was therefore added once more at the C-terminal end of the V5-His6. The Pis1-V5-His6-KXKXX variant of wt Pis1 is named in

the following Pis1-K. The enzymatic activity of Pis1-K was roughly 2 times lower than the one of Pis1 (Fig. 5A, B). The substitution of Cys at position 66 decreased microsomal activity drastically, whereas Cys substitution at positions 69 and 71 increased it or left it intact (Fig. 5A, B), in keeping with what was observed with the analogous substitutions done in the Pis1ΦC background (Fig. 3D). (The strong inactivating effect of the Y66C substitution is somewhat surprising in view of the fact that many different amino acids are found in this position in other CAPTs, including Cys, *e.g.* in phosphatidylserine synthase of *Pelobacter carbinolicus*.)

Analyzing the Pis1-K derived mutant proteins containing the 5 natural plus a 6th Cys in L2–3, SCAM again produced strong evidence for a cytosolic orientation of the CAPT motif. In particular, positions 66, 68, 69, and 71 were strongly derivatized by PEG-mal in the absence of detergent, and each of those positions was also quite accessible to one or several Ub-mals in the absence of detergent. Thus, 26% of Y66C and 23% of Q68C reacted with Ub-KMUS, 24% of V69 with Ub-SM(PEG)$_4$, whereas S71C was practically non-accessible (Figs. 4C, 5C).
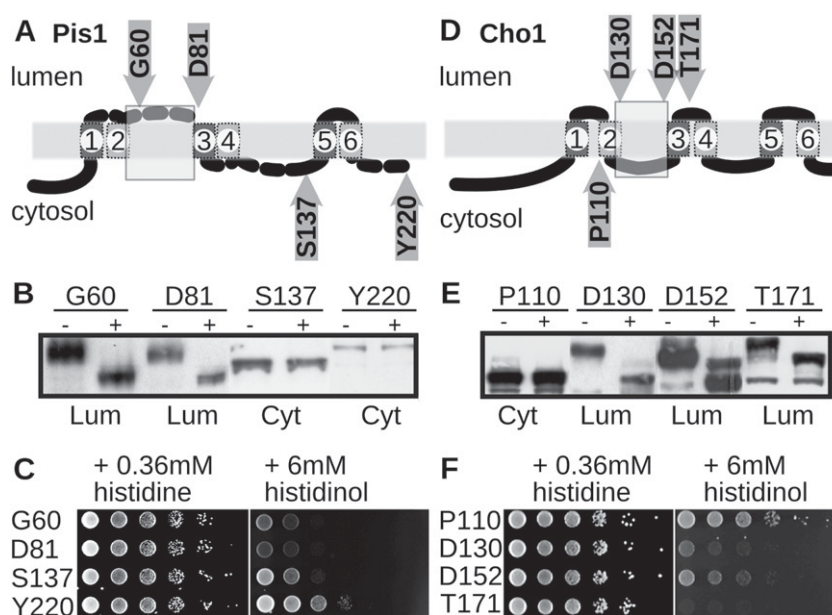
Where direct comparison was possible, it revealed some subtle differences between Cys insertions done in Pis1ΦC and Pis1-K: *E.g.* in the absence of DDM, Cys66 and Cys68 were more accessible to Ub-EMCS in Pis1-K background, whereas the same C66 appeared to be more derivatized by Ub-SM(PEG)$_4$ in Pis1ΦC (Fig. 4C). Another difference concerns the fact that we generally did not observe in the Pis1-K background that 0.05% DDM would make cytosolic Cys residues more accessible (Fig. 4C), but this cannot be substantiated by direct comparison, since we did not use the same Ub-mals were used for a given substitution in the Pis1ΦC and Pis1-K backgrounds. We estimate that these differences are difficult to interpret since we cannot exclude that the Y66C and Q68C substitutions, strongly inactivating the enzyme, would change the protein structure and possibly make one of the native Cys more accessible in one of the two backgrounds but not the other. Thus, we only conclude from these experiments that the CAPT motif also in Pis1-K is clearly cytosolic.

2.7. Probing the CAPT motif by DTR or addition of N-glycosylation sites

Trying to consolidate the above topology of Pis1, a dual topology reporter (DTR) cassette was added at the end of C-terminally truncated

versions of *PIS1*, namely at positions G60, D81, S137 and Y220. This cassette contains an HA tag, a fragment of Suc2 with several confirmed N-glycosylation sites, and His4C, a dehydrogenase required to generate His from histidinol. All constructs yielded unambiguous glycosylation forms. Insertions at G60 and D81, encompassing the CAPT motif of Pis1, were completely glycosylated and didn't grow on histidinol (Fig. 6A–C), suggesting that the CAPT motif is luminal, quite in contrast to the SCAM data. On the other hand, insertions at S137 and at the C-terminal end (Y220) clearly placed loop L4–5 and the C-terminal end into the cytosol, in agreement with SCAM data. The last finding also confirmed earlier DTR data obtained by others [23]. Similarly, DTR experiments also suggested that the CAPT motif of the CDP-diacylglycerol:L-serine O-phosphatidyltransferase (Cho1, Fig. 1) has its CAPT motif on the luminal side of the ER, although TOPCONS places the CAPT motif of Cho1 into the cytosol (Fig. S2B). The performance of the C-terminal reporter approach has been critically evaluated using a crystallized bacterial H$^+$/Cl$^-$ transporter as a model [24]. Correct results were only obtained where the DTR was inserted at a certain distance downstream of a TM having a ΔG for membrane insertion (ΔG$_{mi}$) < 1 kcal/mol (http://dgpred.cbr.su.se/). In our case, TMs 2, 4 and 6 of Pis1 and TMs 1, 2, and 3 of Cho1 preceding the DTR insertions made in Pis1 and Cho1, respectively, all have higher ΔG$_{mi}$ values (not shown). This suggests that, similar to the criteria defined for bacterial plasma membrane proteins [24], the DTR approach is non-reliable in yeast microsomes if these same criteria are not met.

We also tried to consolidate the topology of Pis1 model proposed by TOPCONS (Fig. 1C, line f) by the insertion of N-glycosylation consensus sites NXS/T [16]. NXS sequons were created by site-directed mutagenesis of non-conserved residues in L2–3 (V69S (NQVSS → NQSSS) and V69N (NQVSS → NQNSS)) located in the CAPT motif of Pis1, at a distance of 27–29 residues from the end of the uniformly predicted TM1 (Fig. 1C). Sites were also created in L4–5, namely G133N–G135S (VGEGES → VNESES), G135N (VGEGES → VGENES), and triple substitution at 134–136 (VGEGES → VGNESS). Western blotting showed that neither wt Pis1 nor any of the NXS-containing constructs were N-glycosylated (Fig. S9). This negative result is fully compatible with the cytosolic location of loops L2–3 and L4–5 suggested by SCAM data, but it does not provide firm evidence for such a location, as only about 2/3 of potential N-glycosylation sites are utilized by yeast cells *in vivo*

Fig. 6. Topology by DTR. A, schematic representation of Pis1 according to the topology of TOPCONS PRO with the rather unanimously predicted orientations drawn as solid lines, the ambiguous loops as dotted lines. Residues, where Pis1 was truncated by DTR are pointed by arrows positioned so as to reflect the DTR result. B, DTR constructs are visualized by Western blotting with anti-HA antibodies after treatment with endoglycosidase H (+) or control incubation (−). C, 10-fold dilutions of STY50 cells harboring the DTR-tagged Pis1 constructs on medium supplemented with histidine or histidinol. D–E, as A–C, but for Cho1.

[25]. No phospho-sites, usually cytosolic, have been described in Pis1 according to SGD (http://www.yeastgenome.org/).

3. Discussion

The experiments described here have been performed before June 2014, at a time when the first two crystal structures of CAPTs had not yet been published. Thus, substitutions were made solely based on the TOPCONS predictions. The possibility to model the Pis1 sequence on a crystal structure now allows to interpret SCAM data with higher confidence, although it should be said that the eukaryotic PI synthases are not closely related to the archeal DIPPSs [3] and the model therefore may be somewhat inaccurate, especially as DIPPSs do not use a lipid substrate. Presently, our data orient the yeast Pis1 model of Figs. 1C and 4B with regard to the ER membrane and assign its CAPT motif to the cytosolic side of the ER membrane; they predict structural changes in the CAPT domain following addition of detergent and probe the accessibility of different regions of Pis1 in its natural context. Data also allow to critically appreciate the performance of different SCAM methods as well as of bioinformatic topology predictors.

It clearly appears that bioinformatic predictors have great difficulty to deal with proteins containing deep hydrophilic pockets such as Pis1 because several of its TMs are amphiphilic and have high ΔG_{mi} values. TOPCONS predicts a cytosolic location of the CAPT motif for about 75% of fungal *PIS1* homologs, but a luminal one for a distinct minority comprising *e.g.* Pis1 of *Klyveromyces lactis*, *Coprinopsis cinerea*, *Vanderwaltozyma polyspora* etc. Interestingly, TOPCONS algorithms pretty unanimously predict a wrong topology with 4 TMs and a luminal CAPT motif also for AfDIPPS, as they do for Pis1, whereas for Af2299, the second CAPT of *Archaeoglobus fulgidus* that recently was crystallized [3], is predicted with 6 TMs and a cytosolic CAPT motif (Fig. S10). The failure of TOPCONs with regard to correctly placing the CAPT motif of AfDIPPS and possibly other fungal Pis1 homologs apparently derives from the fact that it does not consider TM2 and TM3 as TMs, most likely because the cytosolic ends of these two TMs are highly amphiphilic, since they comprise the conserved Asp residues of the CAPT motif. The ΔG predictor (http://dgpred.cbr.su.se/) finds all 6 TMs in yeast Pis1, as long as one does not ask for TMs longer than 16 amino acids, which is reasonable in view of current ideas about the thickness of the ER membrane [26].

While the topology of yeast ceramide synthase *LAG1/LAC1* shows that conserved amino acids reside inside the TMs and does not allow to say with certainty on what side of the membrane substrates enter and products emerge [27], the distinct cytosolic location and accessibility of the CAPT motif of Pis1 allow to conclude that substrates and products enter and emerge on the cytosolic side. The Ino substrate for Pis1 is synthesized by the Ino-3-phosphate synthase Ino1 and the phosphatases Inm1 and Inm2, all of which are cytosolic [28]. Similarly, CDP-DAG is produced by Cds1, an integral membrane protein of the ER [29], for which TOPCONS predictors unanimously locate most highly conserved polar residues to the cytosolic side (Fig. S2F). Thus, no membrane transporters for the substrates are required for PI synthesis in yeast. PI itself however will have to flip in order to become a substrate for the inositolphosphorylceramide synthase Aur1 [30].

Activity of detergent solubilized Pis1 can be blocked with the thiol specific alkylating reagent p-chloromercuriphenylsulfonic acid [20]. It is likely that this reaction derivatized one of the Cys that can be derivatized by NEM, Cys154 or Cys53 (Fig. 2C), since, as NEM, this reagent reacts with deprotonated Cys. Cys154 may be the important residue, since Cys154 is more accessible. Also, the C154A mutation causes a drastic reduction of catalytic activity (Fig. 5A, B). It was speculated that the gap in the lateral wall of the central cavity, visible on the front view of Fig. 4B below the short TM5, would allow CDP-DAG to enter the central cavity and therefore may have to transiently or permanently stay open in Pis1 [3]. Thus, alkylation of Cys154 at the beginning of TM5 may prevent CDP-DAG from sliding into the active site. One also can speculate that the generally better activity with CDP-DAG 16:0 than

CDP-DAG 18:1 observed in many mutants points to a reduced size or flexibility of this lateral gate in those mutants (Figs. 3D vs. E; S6).

Association of Pis1 with lipids may be important to maintain the enzymatically active structure because 0.5% of DDM and Triton X-100 completely inactivate the protein, although lower concentrations of DDM seem to slightly activate it. Activation by detergent may reflect a structural change but may also be due to better solubilization of CDP-DAG. An earlier study found good activity of a crude extract at 0.1% Triton X-100, but showed that highly purified Pis1 had best activity at about 0.2% Triton X-100 and maintained significant activity even at 1.6 % Triton [20]. The discrepancy with our findings may partially be explained by the different pH used in the assays, but may also hint at a possible activation of Pis1 by multimerization, which is facilitated in purified Pis1 preparations. Both *A. fulgidus* CAPT enzymes crystallized as homodimers with a symmetric dimer interface formed by TMs 3 and 4. It thus is conceivable that the active form of Pis1 forms such a dimer through hydrophobic interactions of TMs 3 and 4 of one subunit with the same TMs of a second subunit, and that detergent would inactivate the enzyme by dissociating the dimers.

Addition of a KXKXX motif reduced the activity of Pis1 by a factor of 2 (Fig. 5A, B), as if the enzyme had stronger activity in the Golgi. This also may hint at an influence of the lipid environment on Pis1 activity, since the lipid composition of the Golgi is different from the one of ER. Localization studies showed that Pis1 occurs in more than two locations, namely in the ER, the Golgi, and punctate structures [28,31], but these studies have to be regarded with caution as in these studies too, the C-terminal KXKXX had been covered up by the C-terminally added GFP. We presently try to pursue the question of whether the subcellular location of Pis1 has an influence on its specific activity.

Assuming that the general 6 TM topology and orientation of the Pis1 model of Figs. 1D and 4B are correct, our data allow comparing the performance of different SCAM methods and identifying certain pitfalls:

1) It seems that the use of ubiquitin linked to maleimide through crosslinkers of different lengths allows differentiating easily accessible form less accessible residues. Thus, in the absence of DDM, most residues of the CAPT domain of Pis1ΦC were not very accessible to Ub-mals with spacers shorter than 17 Å, whereas residues 132–137 in L4–5 were quite accessible to Ub-EMCS, which has a short 9 Å spacer (Fig. S7B). Similarly, in the presence of 0.05% DDM, some residues, such as L72C became readily accessible even to Ub-GMBS (7 Å spacer) whereas most other residues of the CAPT motif were more accessible to long spacers than shorter ones (Fig. S7B). Thus the differential use of different spacers seems to allow to estimate relative accessibility of residues, which may depend not only on the position of a residue in a given secondary structure and at a given distance from the membrane but also on steric effects of loop structures or peripheral membrane proteins making the access path for maleimides to a given Cys longer.

2) Whereas many Ub-mals did not react very efficiently with residues in the CAPT motif in the absence of DDM, PEG-mal reacted efficiently with about all residues in the CAPT motif (Fig. S7B). Part of this difference may be attributable to the fact that the final concentration of Ub-mals utilized was probably significantly lower than the intended 1 mM, which is the concentration of PEG-mal we used. We believe that the higher efficiency of PEG-mal also is due to other factors, notably to its long thread-like structure, enabling it to reach into the deepest pockets of a protein.

3) In cases where Ub-mals cannot access cytosolic Cys of the CAPT motif and gain access only in the presence of 0.05% DDM (*e.g.* positions 70 or 72), classical interpretation would erroneously place the Cys under question into the ER lumen (Figs. 4, S7B). Such erroneous assignments of residues as being luminal can be avoided by testing multiple sites in a given hydrophilic loop. The caveat may however only be pertinent for membrane proteins, the activity

of which is highly sensitive to detergent. In the case of Pis1, a possible reason for structural changes in the CAPT motif is that mild detergent may purge the endogenous CDP-DAG we know to be present in microsomes (Fig. S5C) from the active site. This may change the configuration of the CAPT motif, which from the 3D structure is known to hold the cytidine ring (see Introduction) [3]. On the other hand, a single residue reacting with Ub-mal (or PEG-mal) in the absence of detergent seems to be sufficient to safely attribute a cytosolic position to a given loop.

4) Cys53 and Cys154, residing according to the model of Fig. 4B close to the bottom of the cytosolic cavity of Pis1, are partially and fully accessible for the small NEM but not for PEG-mal: This suggests that the PEG-mal/NEM method also may attribute erroneously a luminal location when applied to proteins with deep pockets such as Pis1. Again, testing multiple sites avoids the error.

5) That the complete inactivation of Pis1 by 1% DDM is the consequence of a rather drastic loss of 3D structure is supported by the fact that several residues such as K65C, and N67C were strongly derivatized by Ub-EMCS in the presence of 1% DDM, but not at all by Ub-mals with similar spacer length (Ub-GMBS, Ub-SMPB, Ub-KMUS) in the presence of 0.05% DDM.

6) We did not find any case where PEG-mal reached a Cys placed in the ER lumen by the model of Fig. 4B, confirming the general reliability of the PEG-mal/NEM method and arguing that PEG-mal does not glide through the membrane at 4 °C.

Our study also clearly indicates the limits of the DTR methodology, even if it gives clear-cut results, since DTR predicted that the CAPT motif of Pis1 and Cho1 are luminal, which clearly is not the case for Pis1 and which, based on what we learned through this study, we believe to be erroneous with regard to Cho1. The DTR data however may point to the transient residency of L2–3 in the lumen of the ER during translocation through the Sec61 pore, although we could not detect N-glycosylation of artificial glycosylation sites in L2–3 (Fig. S9). Indeed, it will be challenging to study how TM2 of Pis1, having hydrophobic residues only in one half of the TM, is handled by the Sec61 translocon at high chronological and spatial resolution as done recently for other proteins [32].

4. Conclusions

Cytosolically made inositol and CDP-DAG can access the active site of the yeast PI synthase Pis1 from the cytosolic side and Pis1 structure and function is strongly affected by mild detergents. In such detergent sensitive proteins, results obtained by SCAM methods have to be interpreted with care, in order to avoid erroneous assignment of residues to the luminal surface of the ER.

5. Materials and methods

5.1. Yeast strains and growth conditions

Strains and vectors are listed in supplemental Tables S1 and S2, primers for PCR in Table S3. Wt *PIS1* was amplified by PCR from BY4742 genomic DNA and cloned into pYES2NT/B. The 5 cysteines (Cys) of *PIS1* in the resulting PIS1-V5-H6 plasmid were mutated to Ala by site-directed mutagenesis (Agilent Technologies, Stratagene QuikChange II XL or QuikChange Multi), yielding plasmid pis1ΦC-V5-H6. The same method was used to substitute single residues by Cys in the pis1ΦC-V5-H6 or PIS1-K plasmid. All constructs were verified by sequencing at Microsynth, Balgach, Switzerland. Cells were routinely grown in complete synthetic medium, *i.e.* YNB plus drop out mixes, or YPD, containing 2% of glucose, raffinose, or galactose, unless indicated differently.

5.2. In vivo functionality of Pis1

The various constructs derived from plasmid PIS1-V5-H6 were transfected into a diploid *pis1Δ::kanMX/PIS1* strain. In dissected tetrads *pis1Δ* spores were differentiated from *PIS1* spores by their ability to grow on galactose media containing G418 and their concomitant inability to grow on 5′-fluoroorotic acid (FOA). Alternatively PIS1-V5-H6 constructs were introduced into the *pis1Δ/PIS1** strain from which haploid progeny could be obtained using a synthetic genetic array (SGA) selection protocol [33].

For growth assays the *pis1Δ* strains harboring the various PIS1-V5-H6 alleles on plasmids were transferred from galactose plates to liquid galactose medium making them adapt to liquid culture. Then, overnight precultures in YNB containing either glucose, raffinose or galactose were prepared and used to inoculate Bioscreen C (Oy Growth Curves) microtiter plates having the identical media at an OD_{600} of 0.03 (200 μl per well). Plates were incubated at 30 °C for 36 h, during which every 30 min the plates were automatically shaken and the absorption was measured at 600 nm.

5.3. Substituted cysteine analysis method (SCAM)

5.3.1. Induction of Pis1 for SCAM and PI synthase activity

Wt or *pis1Δ* cells containing 2xFLAG-*GPI8* and a Cys variant of *PIS1* on plasmids were routinely precultured at 30 °C in YNB 2% galactose to insure galactose competence. Then, 400 ml cultures of YNB with 0.1% glucose were inoculated at an OD_{600} of 0.03 for SCAM, at 0.01 for activity tests, and grown over-night at 30 °C, until cells reached an OD_{600} of 1–2. The expression of the various Pis1 was induced by adding 2% galactose and incubating the cells for 30 min at 30 °C with shaking.

5.3.2. Microsome preparation

Microsomes from cells grown and induced as above were prepared as described [5], except that cells were washed at RT, treated with zymolyase at 32 °C and lysed at 100 OD_{600} units/ml in lysis buffer. The microsomal pellet was resuspended to a final protein concentration of 3–10 μg/μl and immediately used for the SCAM or PI synthase activity assays. An aliquot of microsomes was quickly frozen in liquid nitrogen and stored at −20 °C for Western blot quantification of Pis1. Microsomal protein content was estimated using the Bradford reagent.

5.3.3. Ubiquitin-maleimide synthesis

25 mg of ubiquitin (2.92 μmol) and 2.4 mg of sulfo-EMCS (5.85 μmol) were dissolved in 760 μl and 870 μl of buffer A (50 mM sodium-phosphate pH 7.2). Both solutions were mixed together and incubated for 30 min at RT, on a rotating wheel. Non-reacted cross-linker was removed from the mixture by two concentration steps (from 0.6 to 0.2 ml) using Vivaspin 500 columns (MWCO 3 kDa) and adding buffer A in between. The dialyzed reaction mixture was adjusted to 3 mM Ub-EMCS in buffer B (43 mM sodium phosphate pH 7.2, 0.2 M sorbitol), aliquoted and stored at −20 °C for use on the next day. The other cross-linkers, sulfo-GMBS, sulfo-KMUS, sulfo-SMPB, SM(PEG)$_2$, and SM(PEG)$_4$ were coupled as above, but at a 1:1 molar ratio of ubiquitin: crosslinker.

5.3.4. Substituted cysteine accessibility method (SCAM)

Fifty micrograms of microsomal proteins prepared as above was resuspended in 100 μl of SCAM reaction buffer (buffer C: 0.2 M sorbitol, 5 mM MgCl$_2$, 100 mM Na-phosphate buffer pH 7.2 with 1 mM PMSF, 1× Roche tablet protease inhibitor mix (EDTA-free), and 4 μg/ml pepstatin A, freshly added) or buffer C containing DDM or SDS (1% final). The samples were incubated for 30 min at 0 °C with gentle occasional shaking to allow for membrane solubilization, except for the samples in SDS, which were kept at RT. 50 μl of 3 mM Ub-EMCS or buffer B was added. Samples were incubated with occasional gentle shaking during 30 min at 0 °C (or RT for the samples in SDS); then the reactions were quenched by adding dithiothreitol (DTT, 25 mM final).

After another 15 min, all samples were heated 15 min at 65 °C in reducing sample buffer (58 mM Tris-HCl pH 6.8, 1.7% SDS, 0.7 M glycerol, 0.1 M DTT, bromphenol blue) and stored at −20 °C. The same protocol was followed when using other crosslinkers, except that the experiments were downscaled by half (25 μg of microsomal proteins) and DDM reduced to 0.05% w/v, which turned out to be sufficient to open the microsomes. Using an alternative method [8,17], we added to microsomes 0, 0.3 or 5 mM of the membrane-permeating alkylation reagent NEM for 30 min at RT. The derivatized microsomes (100 μg) were washed twice in ice-cold buffer C without detergent (30 min, 4 °C, 16,000 ×g) then incubated for 15 min at 0 °C with 1 mM (final) PEG-mal before addition of SDS (0.5% final) and further incubation for 25 min at RT. The reactions were quenched by adding 25 mM DTT for 15 min, addition of reducing sample buffer and heating, as above.

5.3.5. Western blot analysis

Standard procedures were used as detailed in supplemental methods section. Antibody-labeled proteins were visualized by ImageQuant LAS400 (GE Healthcare) set on automatic exposure. Bands in each lane were quantified over the same surface using ImageJ 1.46a (http://imagej.nih.gov/ij). The ubiquitinylated fraction in each lane was calculated as percent of the total signal from derivatized and non-derivatized Pis1 bands according to (Pis1$_{deriv.}$ / [Pis1$_{deriv.}$ + Pis1$_{non-deriv.}$]) × 100. The accessibility of each Cys to a derivatizing agent (in %) was then visualized by building a heatmap with R 3.1.0 (www.r-project.org/index.html) (see supplemental methods).

5.4. In vitro assay of Pis1 activity

Haploid $pis1\Delta$::kanMX harboring a $PIS1$ construct on a plasmid were precultured and induced during 30 min and used for microsome preparation as described above. Microsomes (1 μg/μl, final) were solubilized for 30 min on ice in buffer D (0.2 M sorbitol, 5 mM MgCl$_2$, 100 mM Na-phosphate, pH 7.2) supplemented with 0.1 % DDM.

Substrates CDP-DAG 16:0 or CDP-DAG 18:1 in chloroform (Avanti Polar lipids) and [2-^{3}H(N)]myo-Ino in 10% ethanol (Anawa 0116B, 10–30 Ci/mmol) were dried in a rotary evaporator. Standard assays (final volume: 200 μl) contained from 4 to 64 μg (1.2–16 mol.%) CDP-DAG, 1 μCi [^{3}H]myo-Ino (supplemented with cold Ino to final concentrations of 15–240 μM), 100 μl of solubilized microsomes (100 μg) and a final concentration of 0.05% DDM (w/v). The 4–64 μg CDP-DAG corresponds to 1.2–16 mol.%, $i.e.$ 1.2 % of the sum of [nmol of microsomal lipids + nmol of detergent + nmol of CDP-DAG]. They were incubated for 25 min at RT, shaking at medium speed (Vortex), then stopped by adding 780 μl of CHCl$_3$:MeOH (2:1) and vortexing vigorously. The stopped reactions were centrifuged 5 min at 12,000 ×g. The lower organic phase was transferred to a new 1.5 ml plastic tube and was washed by adding 380 μl of the aqueous upper phase of a CHCl$_3$:MeOH:water (26:13:10) mixture, vortexing and centrifugation. The washing was repeated once and the final organic phase (400 μl) was transferred to a new tube. 10% aliquots were taken for scintillation counting. In all assays we ran a control containing microsomes boiled at 95 °C for 10 min, to which 300 μM CDP-DAG and 240 μM cold Ino were added. This control usually produced around 20–70 cpm (0.007% of added radioactivity) and is reported in all assays. To calculate activity, the microsomes used for the assay were analyzed by Western blotting and activity normalized with regard to immunodetected Pis1-V5-His6 as detailed in the supplemental section. The specific activity of [^{3}H]Ino after dilution with cold Ino was used to calculate the nmol of inositol incorporated.

5.5. Modeling of Pis1 structure

A model for Pis1 was created by HHpred and Modeller (http://toolkit.tuebingen.mpg.de/hhpred) based on the known PDB structure

4MND of AfDIPPS (http://pdb.rcsb.org/pdb/). The final alignment was performed with MacPymol using AfDIPPS as a template.

5.6. DTR analysis

The DTR cassette was added at the end of C-terminally truncated versions of $PIS1$ and $CHO1$ by homologous recombination in STY50 cells as described [5,34]. All DTR constructs were verified by sequencing. Growth of the transformed cells was assessed by spotting ten-fold dilutions of cells on YNB 2% glucose plates supplemented by either 0.36 mM histidine or 6 mM histidinol and incubating for three days at 30 °C. The N-glycosylation status of the $SUC2$ fragment was determined by preparing microsomes, and treating 50 μg of TCA-precipitated microsomal proteins with endoglycosidase H (2.5 U), followed by Western blotting with anti-HA antibodies.

List of abbreviations used

CAPT	CDP-alcohol phosphatidyltransferase
CDP-DAG	CDP-diacylglycerol
DAG	diacylglycerol
DDM	dodecylmaltoside
ΔG_{mi}	ΔG for membrane insertion
DIPPS	di-myo-Ino-1,3-phosphate-1′-phosphate synthase
DTR	dual topology reporter
DTT	dithiothreitol
Ino	inositol
NEM	N-ethylmaleimide
PA	phosphatidic acid
PEG-mal	polyethyleneglycol$_{5000}$-maleimide
PI	phosphatidylinositol
Pis1ΦC	Cys-free version of Pis1
RT	room temperature
SCAM	substituted cysteine accessibility method
TM	transmembrane helix
Ub-mal	ubiquitin-maleimide
wt	wild type.

Competing interests

There are no competing interests.

Authors' contributions

The experimental work except for data in Fig. 6 was carried out by A.B.; A.B. and A.C. jointly covered all other aspects.

Appendix A. Supplementary data

Supplementary data to this article can be found online at http://dx.doi.org/10.1016/j.bbalip.2015.02.006.

References

[1] S.A. Henry, S.D. Kohlwein, G.M. Carman, Genetics 190 (2012) 317–349.
[2] J.G. Williams, C.R. McMaster, J. Biol. Chem. 273 (1998) 13482–13487.
[3] G. Sciara, O.B. Clarke, D. Tomasek, B. Kloss, S. Tabuso, R. Byfield, R. Cohn, S. Banerjee, K.R. Rajashankar, V. Slavkovic, J.H. Graziano, L. Shapiro, F. Mancia, Nat. Commun. 5 (2014) 4068.

[4] P. Nogly, I. Gushchin, A. Remeeva, A.M. Esteves, N. Borges, P. Ma, A. Ishchenko, S. Grudinin, E. Round, I. Moraes, V. Borshchevskiy, H. Santos, V. Gordeliy, M. Archer, Nat. Commun. 5 (2014) 4169.

[5] M. Pagac, H.V. de la Mora, C. Duperrex, C. Roubaty, C. Vionnet, A. Conzelmann, J. Biol. Chem. 286 (2011) 36438–36447.

[6] M. Pagac, H.M. Vazquez, A. Bochud, C. Roubaty, C. Knopfli, C. Vionnet, A. Conzelmann, Mol. Microbiol. 86 (2012) 1156–1166.

[7] V. Choudhary, N. Jacquier, R. Schneiter, Commun. Integr. Biol. 4 (2011) 781–784.

[8] Q. Liu, R.M. Siloto, C.L. Snyder, R.J. Weselake, J. Biol. Chem. 286 (2011) 13115–13126.

[9] S.E. Horvath, L. Bottinger, F.N. Vogtle, N. Wiedemann, C. Meisinger, T. Becker, G. Daum, J. Biol. Chem. 287 (2012) 36744–36755.

[10] A.M. Vacaru, J. van den Dikkenberg, P. Ternes, J.C. Holthuis, J. Biol. Chem. 288 (2013) 11520–11530.

[11] A. Bernsel, H. Viklund, A. Hennerdal, A. Elofsson, Nucleic Acids Res. 37 (2009) W465–W468.

[12] J.A. Brito, N. Borges, H. Santos, M. Archer, Acta Crystallogr. Sect. F: Struct. Biol. Cryst. Commun. 66 (2010) 1463–1465.

[13] S. Sanyal, A.K. Menon, ACS Chem. Biol. 4 (2009) 895–909.

[14] S. Vehring, L. Pakkiri, A. Schroer, N. Alder-Baerens, A. Herrmann, A.K. Menon, T. Pomorski, Eukaryot. Cell 6 (2007) 1625–1634.

[15] Z.Y. Guo, S. Lin, J.A. Heinen, C.C. Chang, T.Y. Chang, J. Biol. Chem. 280 (2005) 37814–37826.

[16] A. Bochud, N. Ramachandra, A. Conzelmann, Biochem. Soc. Trans. 41 (2013) 35–42.

[17] Y. Wang, M. Toei, M. Forgac, J. Biol. Chem. 283 (2008) 20696–20702.

[18] M.J. Kelley, A.M. Bailis, S.A. Henry, G.M. Carman, J. Biol. Chem. 263 (1988) 18078–18085.

[19] S.H. Han, G.S. Han, W.M. Iwanyshyn, G.M. Carman, J. Biol. Chem. 280 (2005) 29017–29024.

[20] A.S. Fischl, G.M. Carman, J. Bacteriol. 154 (1983) 304–311.

[21] G.M. Carman, A.S. Fischl, Methods Enzymol. 209 (1992) 305–312.

[22] G.P. Mommen, B. van de Waterbeemd, H.D. Meiring, G. Kersten, A.J. Heck, A.P. de Jong, Mol. Cell. Proteomics 11 (2012) 832–842.

[23] H. Kim, K. Melen, M. Osterberg, G. von Heijne, Proc. Natl. Acad. Sci. U. S. A. 103 (2006) 11142–11147.

[24] M. Cassel, S. Seppala, G. von Heijne, J. Mol. Biol. 381 (2008) 860–866.

[25] M. Aebi, Biochim. Biophys. Acta 1833 (2013) 2430–2437.

[26] H.J. Sharpe, T.J. Stevens, S. Munro, Cell 142 (2010) 158–169.

[27] N. Kageyama-Yahara, H. Riezman, Biochem. J. 398 (2006) 585–593.

[28] M. Breker, M. Gymrek, M. Schuldiner, J. Cell Biol. 200 (2013) 839–850.

[29] Y. Tamura, Y. Harada, S. Nishikawa, K. Yamano, M. Kamiya, T. Shiota, T. Kuroda, O. Kuge, H. Sesaki, K. Imai, K. Tomii, T. Endo, Cell Metab. 17 (2013) 709–718.

[30] T.P. Levine, C.A. Wiggins, S. Munro, Mol. Biol. Cell 11 (2000) 2267–2281.

[31] K. Natter, P. Leitner, A. Faschinger, H. Wolinski, S. McCraith, S. Fields, S.D. Kohlwein, Mol. Cell. Proteomics 4 (2005) 662–672.

[32] P.K. Devaraneni, B. Conti, Y. Matsumura, Z. Yang, A.E. Johnson, W.R. Skach, Cell 146 (2011) 134–147.

[33] A. Baryshnikova, M. Costanzo, S. Dixon, F.J. Vizeacoumar, C.L. Myers, B. Andrews, C. Boone, Methods Enzymol. 470 (2010) 145–179.

[34] H. Kim, Q. Yan, G. Von Heijne, G.A. Caputo, W.J. Lennarz, Proc. Natl. Acad. Sci. U. S. A. 100 (2003) 7460–7464.